

High Performance Sub-Diffraction Limit Three Channel Plasmonic Demultiplexer

Fatemeh Davoodi and Nosrat Granpayeh*

Center of Excellence in Electromagnetics, Faculty of Electrical Engineering, K.N. Toosi University of Technology, Tehran, Iran

*Corresponding Author: granpayeh@eetd.kntu.ac.ir

Abstract— We have proposed a new ultra-compact optical demultiplexer based on metal-insulator-metal plasmonic waveguides aperture-coupled to the ring resonators. Our proposed device has high performance, small footprint, and high potential for integration and development to more channels.

KEYWORDS: High performance Coupling; Plasmonic Ring Resonator; Plasmonic Demultiplexer, Multi Channel Plasmonic Filter.

I. INTRODUCTION

The metal-insulator-metal (MIM) plasmonic waveguides have been taken into consideration, due to their ability to confine the lightwave under the diffraction limit [1-5]. Plasmonic Lens [6], resonators [7] as an essential part of filters [8-11], multi/demultiplexers [12, 13], and routers [14] are widely used. Also, some forms of coupling in resonators and their transmission characteristics have been investigated [15, 16]. Resonators have important role in the optical communication systems and networks [17]. Different kinds of filters have been proposed based on Bragg grating filters [18, 19] and tooth-shaped plasmonic waveguides [20]. Because of required large number of periods in Bragg grating, the sizes of these kinds of filters are too large. The bandwidth of the tooth-shaped plasmonic filters is too broad to be suitable for WDM applications.

Ring resonators are appropriate elements for using in the plasmonic filters. Various shapes of plasmonic ring resonators such as universal ring resonators, racetrack resonators have been proposed and analyzed. The universal plasmonic ring resonators suffer from low coupling of power to the ring, therefore their extinction ratios are low. The coupling power of the ring to the waveguide depends on different factors such as coupling length and injected power. In the racetrack resonators, utilizing a short round trip length helps to increase coupling power between resonator and waveguide in add-drop and band stop devices. Due to the considerable loss in the MIM plasmonic waveguides, the length cannot be so large. To attain high performance in this type of resonator, a tradeoff between plasmonic loss and coupling coefficient is required. The free spectral range (FSR) of the racetrack resonator is low in compared to the universal one [21]. Aperture-coupled ring resonators are more applicable, due their wide FSR and enhancement of coupling power by their apertures compared to the universal plasmonic ring resonators [15].

The resonance frequencies of the plasmonic ring resonators depend on their geometrics, dielectric constants, and radii. Increasing the dielectric constant of the ring resonators core, increases the concentration of the electromagnetic fields in the resonators, as a result, the same resonance frequency is attained for smaller radii of ring plasmonic ring resonators with higher core indices.

Therefore, the quality factor of the resonator increases and its footprint decreases.

To eliminate low coupling power of the waveguide to the ring resonator, we have used aperture coupling structure. In this way, the power between the bus waveguide and the ring resonator is coupled through an aperture cut in the gap between the ring resonator and the waveguide which is assumed thicker than skin depth of silver at the wavelength of $1.55 \mu\text{m}$ to assure that the evanescent waves to be disappeared in the lossy metal gap between the ring resonator and the waveguide.

Due to the lossy nature of plasmonic waveguides, the power is dissipated in the way from source to the ring resonator. The ring resonator, which is located farther from the source, receives lower power. Amplification of the electric and the magnetic fields in the ring resonators depend on the input power of the ring resonator and this affect the intensity of the fields in the output.

In the similar models with the same dielectric constants of the ring resonators, due to the metal losses, the optical power of the second and the third resonators are weak and because of the weak coupling coefficient of plasmonic, the aperture-coupled MIM ring resonators could not be extended to other applicable devices. To compensate this phenomenon, we have used different dielectric constants in the rings. We have increased the dielectric constant for the rings farther from the source. Assignment of higher dielectric constant to the ring resonators, farther from source, cause has the same power at different output ports.

In the other word, we use a creative method to compensate the reduction of energy in the farther resonators, which receive lower energy. In our method, the permittivities of the farther resonators are increased. So, the confinement of the propagating energy in the resonance wavelength is improved and the drop of intensity because of the lossy nature of the plasmonic structure is compensated by increasing the lightwave coupled to the ring

resonator and hence the quality factor of the ring resonator is increased.

II. THEORETICAL ANALYSIS

The environment of plasmonic ring resonator is about several hundred nanometers. Light can be coupled from the waveguide to the ring resonator by evanescent waves through the metallic gap between the ring resonator and the waveguide. Since rings have closed structure, they can be used as resonator devices. Optical waves in special frequencies can intensify and remain in the ring. The resonance frequency of the ring resonators, depend on some factors. Length of optical path should be multiple of resonance wavelength in the ring. This is shown in (1) [15]:

$$m\lambda_m = 2\pi R n_{eff} \quad (1)$$

As here λ_m is the wavelength of longitudinal mode number m , R is the ring radius and n_{eff} is the effective refractive index of the MIM plasmonic waveguide. The rings resonate at different frequencies by changing the optical path length. This occurs when n_{eff} is changed. n_{eff} depends on effective width and the core index of MIM waveguide. We have used the dispersion relation of surface plasmon polariton for TM modes in MIM waveguides to compute n_{eff} of the waveguide. Surface plasmon polariton dispersion relation is shown in Eq. (2) [22].

$$\frac{\varepsilon_d p}{\varepsilon_m K} = \frac{1 - \exp(kd)}{1 + \exp(kd)} \quad (2)$$

where $k = (\beta_{gspp}^2 - \varepsilon_d k^2)^{\frac{1}{2}}$ and

$p = (\beta_{gspp}^2 - \varepsilon_m k^2)^{\frac{1}{2}}$. β_{gspp} and k are propagation constant of plasmon polaritons and wave number, respectively. ε_m and ε_d are dielectric constant of metal and insulator used in MIM waveguide. The metallic sidewalls are assumed silver. We used Drude model to introduce the dispersive behavior of silver permittivity at infrared frequencies. We use

experimental data of [23] for Drude model of silver to achieve a good approximation for silver permittivity at infrared frequency range. The permittivity function of silver is [22]:

$$\varepsilon_r = \varepsilon_\infty - \frac{\omega_p^2}{\omega^2 + j\gamma\omega} \quad (3)$$

where for silver $\varepsilon_\infty = 3.7$, $\omega_p = 1.3826 \times 10^{16}$, and $\gamma = 2.7348 \times 10^{13} \text{ s}^{-1}$. Dielectric core of the waveguide is assumed to be a special kind of polymer with refractive index of 1.6 at infrared wavelengths. We used Eq. (2) and derived the effective refractive index of waveguide in three different widths of 100 nm, 70 nm, and 50 nm. The results are shown in Table 1.

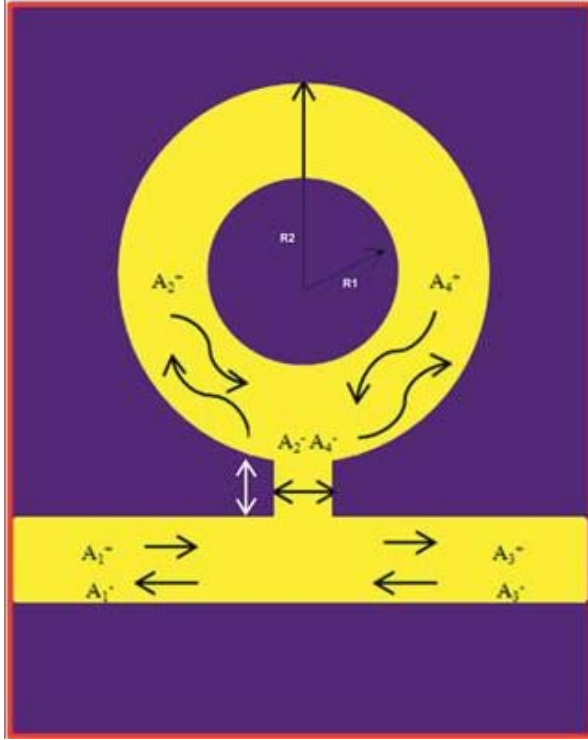


Fig. 1. The aperture-coupled ring and waveguide fields considered for theoretical modeling

The aperture-coupled ring and waveguide fields considered for theoretical modeling are demonstrated in Fig. 1. In aperture-coupled, we have used the effective refractive indices derived from Eq. (2). Aperture-coupled ring resonators are analyzed based on the hole coupler theory. Regardless of evanescent coupling waves, the small aperture can be

simulated with electric and magnetic dipoles radiating to bus waveguide [1].

Table 1 Effective refractive Index of three different width of MIM waveguide.

Width of waveguide	Effective refractive index
100 nm	1.827792688-j0.0017712737
70 nm	1.875161291-j0.0018129065
50 nm	1.905508305-j0.0019055083

The dispersion matrix of the aperture-coupled model of device of Fig. 1 with assumption of $k_f = k_r = k$ is as below, we have modified the Yariv's and Amarnath's models of the semiconductor devices [24, 25], for the lossy plasmonic medium:

$$\begin{bmatrix} A_1^- \\ A_2^- \\ A_3^- \\ A_4^- \end{bmatrix} = \begin{bmatrix} s_{11} & s_{12} & s_{13} & K \\ s_{21} & s_{22} & K & s_{23} \\ s_{31} & K & s_{33} & s_{34} \\ K & s_{42} & s_{43} & s_{44} \end{bmatrix} \begin{bmatrix} A_1^+ \\ A_2^+ \\ A_3^+ \\ A_4^+ \end{bmatrix} \quad (4)$$

According to mode theory model in Bethe holes couplers $K = jk$ and $t = \tau - jk$ [26]. According to matrix orthogonality, Eqs. (4) and (5) can be applied to matrix (4).

$$|s_{11}|^2 + |s_{12}|^2 + |s_{13}|^2 + |s_{14}|^2 = 1 \quad (5)$$

$$\tau^2 + 4k^2 = 1 \quad (6)$$

So we can simplify the matrix equation (4):

$$\begin{bmatrix} A_1^- \\ A_2^- \\ A_3^- \\ A_4^- \end{bmatrix} = \begin{bmatrix} jk & -jk & t & -jk \\ -jk & jk & -jk & t \\ t & -jk & jk & -jk \\ -jk & t & -jk & jk \end{bmatrix} \begin{bmatrix} A_1^+ \\ A_2^+ \\ A_3^+ \\ A_4^+ \end{bmatrix} \quad (7)$$

It is a good approximation, to assume no reflected power from the end of bus waveguide, so $A_3^+ = 0$. Using the real and imaginary part of effective refractive index of the plasmonic waveguide based on equation (2) and like Table I, we calculated transmission and reflection coefficients. Based on this assumption and Fig. 1, we achieved the

mathematical relation of the elements of matrix (7):

$$A_2^+ = A_4^- a_{rt} e^{-\varphi_{rt}} \quad (8)$$

$$A_4^+ = A_2^- a_{rt} e^{-\varphi_{rt}} \quad (9)$$

where φ_{rt} and a_{rt} are the rotation phase in the ring and the attenuation of the amplitude in one turn of lightwave travel in the ring, utilizing (2), (10), (11), and (12) the parameters can be calculated based on the effective refractive index of the device:

$$\beta = \beta' - j\beta'' \quad (10)$$

$$a_{rt} = \exp(2\pi R\beta'') \quad (11)$$

$$\varphi_{rt} = \exp(2\pi R\beta') \quad (12)$$

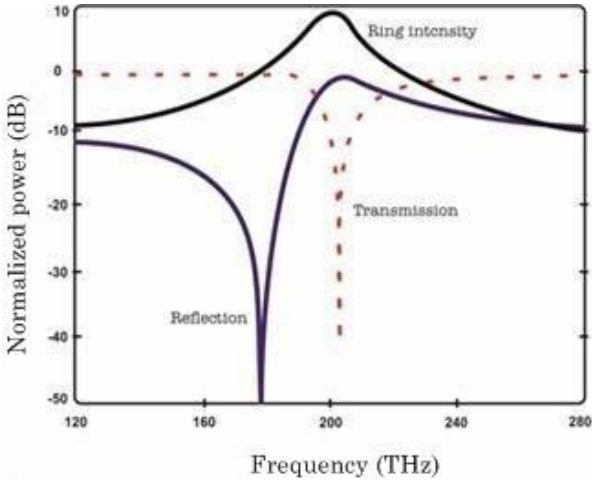


Fig. 2. The theoretical spectra of transmission, reflection, and ring intensity of the structure of Fig. 1. The ring radius is 500nm.

The relation of dispersion matrix (7) can be rewritten in four equations of (13)-(16) as below:

$$A_1^- = jkA_1^+ - jkA_4^- a_{rt} e^{-\varphi_{rt}} - jkA_2^- a_{rt} e^{-\varphi_{rt}} \quad (13)$$

$$A_2^- = jkA_1^+ + jkA_4^- a_{rt} e^{-\varphi_{rt}} + tA_2^- a_{rt} e^{-\varphi_{rt}} \quad (14)$$

$$A_3^- = tA_1^+ - jkA_4^- a_{rt} e^{-\varphi_{rt}} - jkA_2^- a_{rt} e^{-\varphi_{rt}} \quad (15)$$

$$A_4^- = -jkA_1^+ + tA_4^- a_{rt} e^{-\varphi_{rt}} + jkA_2^- a_{rt} e^{-\varphi_{rt}} \quad (16)$$

To achieve the transmission and reflection frequency spectra of the bus waveguide of plasmonic device of Fig. 1, we should use;

$$T_r = \frac{A_4^-}{A_1^+} \quad (17)$$

$$T_t = \frac{A_3^-}{A_1^+} \quad (18)$$

By utilizing Eqs. (13)-(16), analytical Eqs. (19) and (20) will be derived for T_r and T_t :

$$T_r = \left(jk - \frac{2k^2 a_{rt} e^{-\varphi_{rt}}}{1 - \tau a_{rt} e^{-\varphi_{rt}}} \right) \quad (19)$$

$$T_t = \left(t - \frac{2k^2 a_{rt} e^{-\varphi_{rt}}}{1 - \tau a_{rt} e^{-\varphi_{rt}}} \right) \quad (20)$$

Figure 2 depicts the results of the analytical derivation of transmitted and reflected power spectral of the plasmonic bus waveguide near the coupling aperture and the intensity of the power in the plasmonic aperture-coupled ring resonator of the device.

The zero reflected power of the plasmonic band stop filter is because of the diffraction of lightwave from the apertures and the interference of the reflection and transmission power in the bus, its frequency and depth of which change if the distance from the aperture is varied. This phenomenon will be discussed in the next Section.

III. RESULTS AND DISCUSSION

We simulated the band stop plasmonic device of Fig. 1 by two-dimensional FDTD method using convolutional perfectly matched layer (CPML) boundary conditions [27]. The loss of the CPML is -90 dB which is appropriate for simulation infinite space. The metallic side walls are assumed to be silver. The core index of ring resonator with radius $R=500$ nm is 1.6 which belongs to a polymer at infrared

wavelengths. We have used Drude model to simulate the dielectric function of silver, the parameters of which are given following Eq. (3).

The central waveguide has 100 nm width. The thickness of ring is also 100 nm. We used 50 nm apertures and chose 50 nm gap between the waveguides and the rings to assure that the evanescent modes disappeared and the coupling is due to the apertures. The schematic view of the aperture-coupled MIM plasmonic band stop filter is shown in the Fig. 3 and the results of simulations are shown in Figs. 4 and 5.

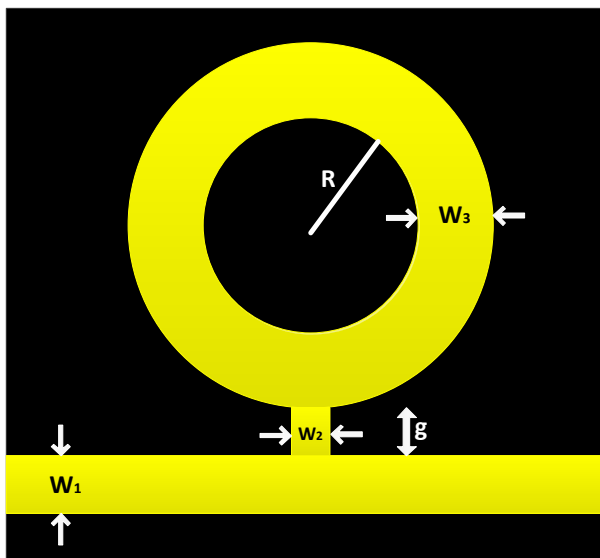


Fig. 3 The schematic view of the aperture-coupled MIM plasmonic band stop filter.

Comparing Figs. 2, 4 and 5, approves that the result of analytical analysis comply very well with those of the simulation ones.

We sampled the reflection in the plasmonic bus waveguide in different distances from the aperture to show the dependence of zero reflection to the location of sampling, the results of which are shown in Fig. 6.

Referring to the result of [15], using two holes improves the coupling power of waveguide to the plasmonic ring resonator through the aperture and amends the reflected power in the bus waveguide propagating toward the input. Utilizing this supposition, we simulated two

kinds of demultiplexer and achieved acceptable results.

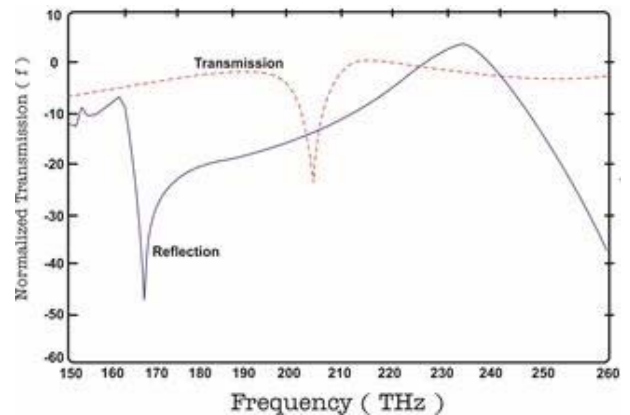


Fig. 4. The schematic view of the aperture-coupled MIM plasmonic band stop filter.

Figure 7 shows the schematic view of our proposed two-channel proposed MIM plasmonic demultiplexer. The device consists of two ring resonators which side coupled to a MIM plasmonic waveguide via two apertures. The apertures are separated by a distance of $\lambda/4$ at central wavelength of $1.55\mu\text{m}$. This multiplexer has several preferences over the similar devices. The device solves the problem of low coupling of ring resonators to MIM waveguide by utilizing the two small apertures [15].

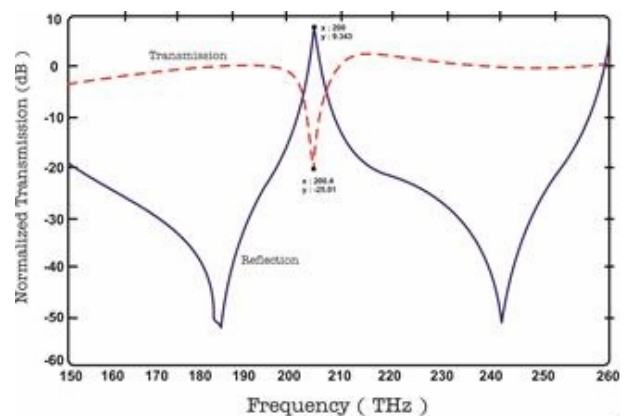


Fig. 5. The spectra of the ring intensity inside plasmonic resonator (solid blue line) and transmission (dashed red line) of structure of Fig. 3.

The coupling power to the ring resonators and as a result the received power at the outputs depends on the coupling coefficient. In the similar add-drop plasmonic ring resonators,

the lightwave is coupled by the evanescent waves through the lossy metallic gap, therefore the performance is low and the loss is high. Using multi aperture theory in this device decreases the reflection power, and increases the extinction ratio at the outputs.

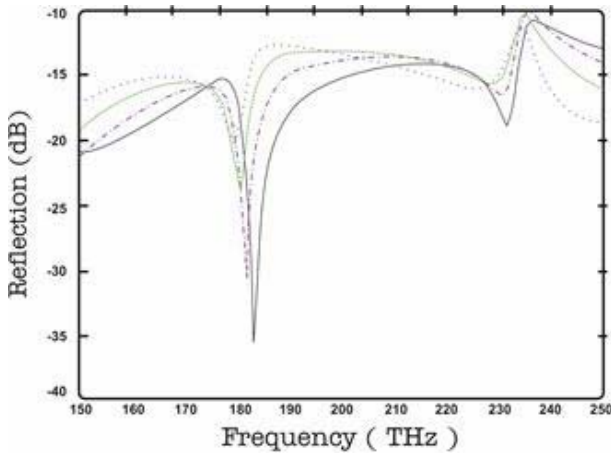


Fig. 6. The reflection power of the plasmonic bus waveguide in different distances from the aperture.

We have proposed a new two-channel MIM plasmonic demultiplexer using two aperture-coupling. The schematic view of this demultiplexer is shown in Fig. 7.

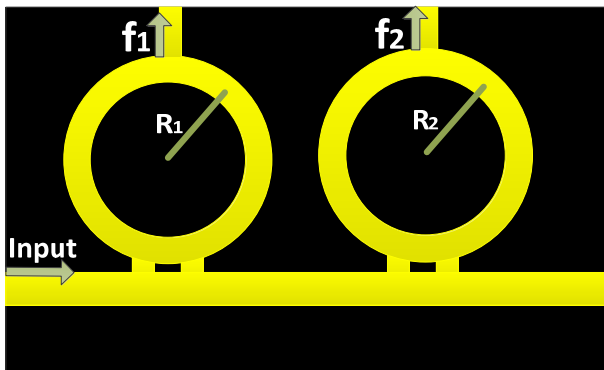


Fig. 7. The schematic view of our proposed two-channel MIM plasmonic demultiplexer.

We simulated structure by two-dimensional (2D)-FDTD method using convolutional perfectly matched layer (CPML) boundary conditions. The metallic sidewalls are assumed silver. The refractive index of the rings core is 1.6 which belongs to some polymer at infrared wavelengths. The ring resonators radii are $R_1=500$ nm and $R_2=550$ nm. We have used the Drude model to simulate the dielectric

function of the silver. The central waveguide and the output waveguides have 100 nm and 70 nm widths, respectively. The widths of rings are also 100 nm. We have used 50 nm apertures and choose 50 nm gap between the waveguides and the rings to assure that the evanescent modes disappeared and the lightwave is coupled through the apertures.

Table 2 Simulated Band Stop Filter Parameters shown in Fig. 3.

Band Stop Filter Parameters	(nm)
R	500
g	50
W1	100
W2	50
W3	100

The input signal including frequencies of $f_1=189.1$ THz and $f_2=216.49$ THz is launched to the demultiplexer. Frequencies of f_1 and f_2 are coupled to the first and the second rings. The other wavelengths are transmitted through the main MIM waveguide. Field distributions of the demultiplexer, wavelength selection of each ring resonator and the transmitted output powers to related output are demonstrated in Figs. 9(a) and 9(b).

The second device we proposed and simulated is a three channel demultiplexer as shown in Fig. 10. The device can drop three frequencies at three different frequency bands that can be used in Gigabit passive optical networks (GPON). This device is customized for GPON application. The device consists of three ring resonators which side coupled to a MIM plasmonic bus waveguide via twin apertures. The twin apertures are separated by a distance of $\lambda/4$ at central wavelength of $1.55 \mu\text{m}$; so the coupling between the adjacent apertures in one resonator is negligible. Utilizing the twin apertures increases the coupling coefficient of the device. The coupling between the adjacent resonators is also negligible, because there is more than 100nm space between them, while the penetration depth of the lightwave in silver is about 20nm; therefore, we have no concern

about the effects of evanescent coupling in our proposed device.

Because of lossy nature of plasmonic waveguides, power is dissipated in the way from source to the ring resonator. The ring located far from the source receives lower power. Amplification of the electric and magnetic fields in the ring resonators depends on their input powers and these affect the intensity of the fields in the outputs. To compensate this phenomenon, we have used different dielectric materials in the rings. The rings located far from the source have higher dielectric constant and the material with high dielectric constant is assigned to the ring resonator located to the farthest ring resonator from the source. The higher permittivity causes the more confinement of the propagating energy and higher quality factor in the ring resonators. In other word, one of the performance parameters of ring resonator is its quality factor which is proportional to the real part of the effective permittivity of the device and has inverse relationship with the imaginary part of the permittivity. So, ring resonator with higher dielectric constant has better confinement of energy in its resonance wavelength. Therefore, the intensities in the output of splitting waveguides are enhanced.

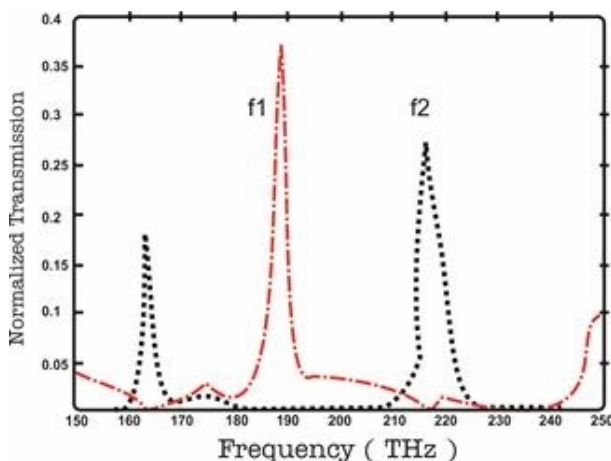


Fig. 8. Output power spectra of the outputs of plasmonic demultiplexer of Fig. 7. The demultiplexed frequencies of $f_1=189.1$ THz and $f_2=216.49$ THz are shown.

As mentioned before, the device solves the problem of low coupling of ring resonators to

MIM waveguide by utilizing two small apertures. Whereas in the similar add-drop plasmonic ring resonators, the lightwave is coupled by the evanescent waves through the lossy metallic gap, therefore the performance is low and the loss is high. The output powers depend on the coupling coefficient between the resonator and the waveguide. Using multi aperture theory in this device decreases the reflection power, increases the extinction ratio at the outputs. Utilizing different materials with appropriate dielectric constants help to attain comparable output levels at different output ports.

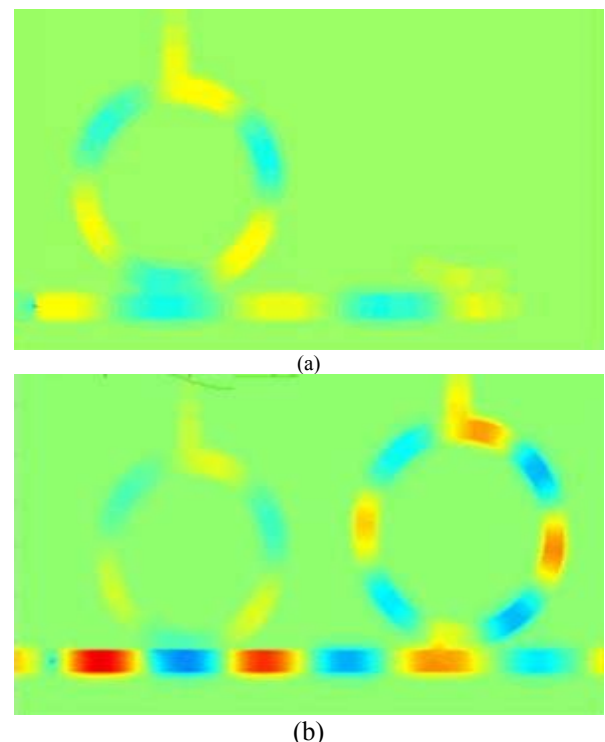


Fig. 9. Field distributions of the plasmonic demultiplexer of Fig. 7, demonstrating the wavelength selection of each ring resonator and the transmitted powers at frequencies of (a) $f_1=189.1$ THz and (b) $f_2=216.49$ THz.

Again, we simulated the three channel plasmonic demultiplexer of Figure 10 by the 2D-FDTD method. The core index of ring resonators with radii $R_1=500$ nm, $R_2=550$ nm, and $R_3=500$ nm, are respectively 1.45, 1.5, and 1.6. Resonators core material with refractive index of 1.45 is SiO₂ and materials with indices of 1.5 and 1.6 belong to two special polymers at infrared wavelengths [21].

We have used Drude model to simulate the dielectric function of silver.

The central waveguide and the output waveguides have 100 nm and 70 nm widths, respectively.

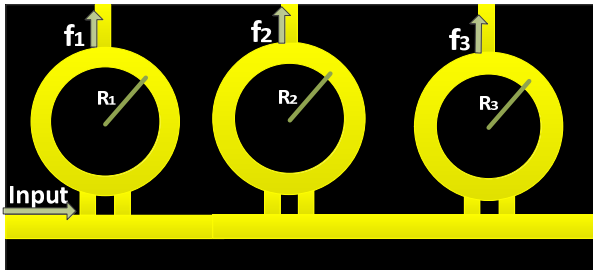


Fig. 10. The schematic view of our proposed three channel aperture-coupled MIM plasmonic demultiplexer.

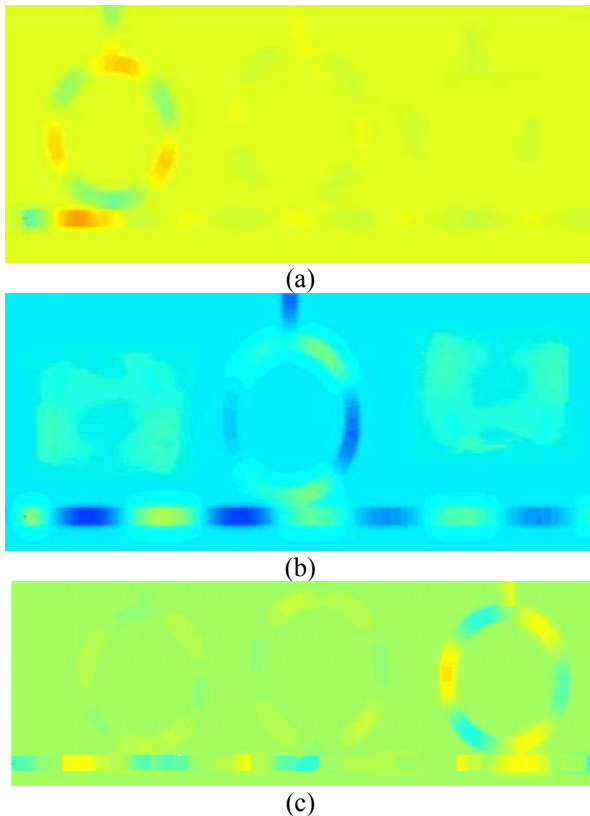


Fig. 11. Wavelength selections of each ring resonator in their resonance wavelengths. The device demultiplexes the frequencies (a) $f_1=189.10$ THz, (b) $f_2=205.00$ THz, and (c) $f_3=216.50$ THz towards different output ports.

The widths of rings are also 100 nm. We used 50 nm apertures and choose 50 nm gap between the waveguides and the rings to assure that the evanescent modes are

disappeared and the coupling is due to the apertures. The field distributions of the demultiplexer, wavelength the selection of each ring resonator and transmitted output powers to related outputs are illustrated in Fig. 11.

It is easy to develop and expand this kind of demultiplexer to more channels if we can find dielectrics with appropriate dielectric constants.

The frequencies of $f_1=189.10$ THz ($\lambda_1=1586.50$ nm), $f_2=205.00$ THz ($\lambda_2=1463.41$ nm) and $f_3=216.50$ THz ($\lambda_3=1385.68$ nm) are respectively coupled to the first, the second, and the third rings and the other frequencies are transmitted through the central MIM waveguide. The signals at f_1 , f_2 , and f_3 exit from the first, second, and third outputs, respectively. The output spectra are derived by fast Fourier transform of the outputs, the results of which are shown in Fig. 12.

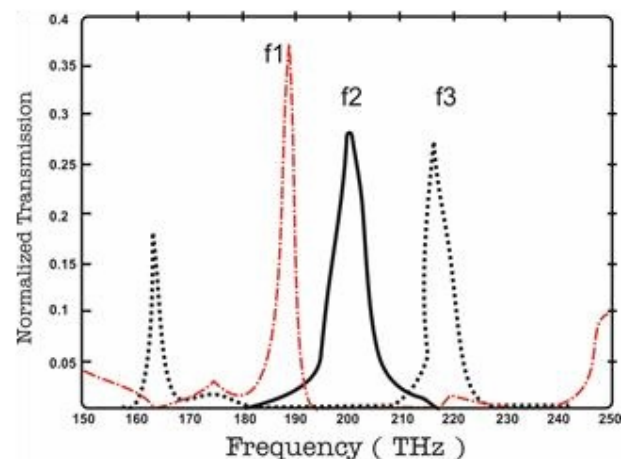


Fig. 12. The output spectra of the proposed three channel MIM plasmonic demultiplexer. The demultiplexed output frequencies of $f_1=189.10$ THz, $f_2=205.00$ THz, and $f_3=216.50$ THz are illustrated.

IV. CONCLUSION

We have proposed the new two and three-channel MIM plasmonic demultiplexers. The conventional plasmonic ring resonator suffers from low coupling power. Some kinds of ring resonators such as racetrack rings and

aperture-coupled rings have been used to enhance the coupling. We proposed aperture-coupled band stop structure to attain good coupling between the ring resonators and the bus waveguide. By utilizing theory of multi hole directional coupler [26], we could attain acceptable coupling, wide free spectral range (FSR), high quality factor, and small footprint of plasmonic structure, which make this device unique. To compensate the loss of plasmonic MIM devices and to obtain comparable output without increasing input power, we used different core materials with different indices in the plasmonic ring resonators.

REFERENCES

- [1] L. Liu, Z. Han, and S. He, "Novel surface plasmon waveguide for high integration," *Opt. Express*, Vol. 13, pp. 6645–6650, 2005.
- [2] K.Y. Kim, A.V. Goncharenko, J.-S. Hong, and K.-R. Chen, "Near-field properties of light emanated from a subwavelength double slit of finite length," *J. Opt. Soc. Korea*, Vol. 15, pp. 196-201 2011.
- [3] Q. Li, and M. Qiu, "Plasmonic wave propagation in silver nanowires: guiding modes or not?," *Opt. Express*, Vol. 21, pp. 8587-8595, 2013.
- [4] J. Jaehoon, and L. Ki-Sik, "Design of Plasmonic Slot Waveguide with High Localization and Long Propagation Length," *J. Opt. Soc. of Korea*, Vol. 16, pp. 305-309, 2011.
- [5] J. Jaehoon and K. Daekeun, "Optimal Design of Dielectric-Filled Plasmonic Slot Waveguide with Genetic Algorithm," *J. Opt. Soc. Korea*, Vol. 16, pp. 70-75, 2011.
- [6] H. Nasari and M.S. Abrishamian, "Active Focusing of Light in Plasmonic Lens via Kerr Effect," *J. Opt. Soc. Korea*, Vol. 16, pp. 305-312, 2012.
- [7] N. Talebi, A. Mahjoubfar, and M. Shahabadi, "Plasmonic ring resonator," *J. Opt. Soc. Am. B*, Vol. 25, pp. 2116-2122, 2008.
- [8] X. Zhou and L. Zhou, "Analysis of subwavelength bandpass plasmonic filters based on single and coupled slot nanocavities," *J. Appl. Opt.* Vol. 52, pp. 480-488, 2013.
- [9] C.J. Yu, "Color filtering using plasmonic multilayer structure," *IEEE 4th International Conf. on Nanoelectronics (INEC)*, pp. 1-2, 2011.
- [10] H. Lu, X. Liu, G. Wang, and D. Mao, "Tunable high-channel-count bandpass plasmonic filters based on an analogue of electromagnetically induced transparency," *J. Nanotechnology*, Vol. 23, pp. 1-6, 2012.
- [11] A. Setayesh, R. Mirnaziry, and M.S. Abrishamian, "Numerical Investigation of Tunable Band-pass\band-stop Plasmonic Filters with Hollow-core Circular Ring Resonator," *J. Opt. Society of Korea*, Vol. 15, pp. 82-89, 2011.
- [12] B. Zhang, J. Guo, and S. Yin, "Multiplexed Plasmonic Nanostructures for Wideband Optical Filters," *J. Opt. Info Base*, 26th meeting on Laser Science, *Frontiers in Optics Conf. Paper JTUA02*, 2010.
- [13] X.Q. Yu and S.N. Zhu, "Wavelength division multiplexer of surface plasmon polaritons using dual-periodical arranged metal gap waveguide," *3rd Conf. Nanoelectronics*, pp. 348-349, 2010.
- [14] S. Papaioannou, K. Vyroskinos, O. Tsilipakos, A. Ptilakis, K. Hassan, J. Weeber, L. Markey, A. Dereux, S.I. Bozhevolnyi, A. Miliou, E.E. Kriezis, and N. Pleros, "A 320 Gb/s-Throughput Capable 2×2 Silicon-Plasmonic Router Architecture for Optical Interconnects," *IEEE J. Lightwave Technol.* Vol. 29, pp. 3185-3195, 2011.
- [15] Z. Han, V. Van, W.N. Herman, and P.T. Ho, "Aperture-Coupled MIM Plasmonic Ring resonator with sub diffraction volumes," *J. Opt. Express*, Vol. 17, pp. 12678-12684, 2009.
- [16] T.B. Wang, X.W. Wen, C.P. Yin, and H.Z. Wang, "The transmission characteristics of surface plasmon polaritons in ring resonator," *Opt. Express*, Vol. 17, pp. 24096-24101, 2009.
- [17] A.R. Dolatabady and N. Granpayeh, "All Optical Logic Gates Based on Two Dimensional Plasmonic Waveguides with Nanodisk Resonators," *J. Opt. Soc. Korea*, Vol. 16, pp. 432-442, 2012.
- [18] Z. Han, E. Forsberg, and S. He, "Surface Plasmon Bragg grating Formed in Metal-Insulator-Metal Waveguides," *IEEE J.*

Photon. Technol. Lett. Vol. 19, pp. 91-93, 2007.

- [19] B. Jafarian, N. Nozhat, and N. Granpayeh, "Analysis of a Triangular-shaped Plasmonic Metal-Insulator-Metal Bragg Grating Waveguide," J. Opti. Soc. Korea, Vol. 15, pp. 118-123, 2011.
- [20] X. Lin and X. Huang, "Tooth-shaped Plasmonic Waveguide Filters with Nanometric Sizes," J. Opt. Lett. Vol. 33, pp. 2874-2876, 2008.
- [21] Z. Han, "Ultracompact Plasmonic Racetrack Resonators in Metal-Insulator-Metal Waveguides," J. Photon. and Nanostruct.-Fundamentals Appl. Vol. 8, pp. 172-176, 2010.
- [22] S.A. Maier, *Plasmonics, Fundamentals and Application*, Springer, 2007.
- [23] P. Johnson and R. Christy, "Optical Constants of the Noble Metals," J. Phys. Rev. B, Vol. 6, pp. 4370-4379, 1972.
- [24] A. Yariv, "Universal relations for coupling of optical power between microresonators and dielectric waveguides," J. Electron. Lett. Vol. 36, PP. 321-322, 2000.
- [25] K. Amarnath, *Active microring and microdisk optical resonator on Indium Phosphide*, PhD dissertation, University of Maryland, College Park, 2006.
- [26] A. Das and S.K. Das, *Microwave engineering*, Tata McGraw-Hill Education, 2000.
- [27] A. Taflove and S.C. Hagness, *Computational electromagnetic: the finite-difference time-domain method*, Artech House, 2005.



Fatemeh Davoodi was born in Tehran, Iran on January 09, 1986. She received her B.Sc. degree in Electronic in Electrical Engineering from Isfahan University, Isfahan, Iran, in

2008, and M.Sc. degree in Fields and Waves in Communication Engineering from K.N. Toosi University of Technology, Tehran, Iran, in 2011. She started studying as Ph.D. candidate in Fields and Waves Engineering at K. N. Toosi University of Technology in 2013.

She has worked as lecturer at department of Electrical Engineering of Azad University and as test manager on Gigabit Passive Optical Network (GPON) in ITRC for one year. She is also an expert in SDH and WDM Laboratory of ITRC and as a verifier of high speed electronic integrated circuit in APAT Company. Her research fields of interest include all-optical logic gates, Plasmonic circuits, optical nonlinear effects, and GPON tests. She is a member of IEEE and OPSI.



Nosrat Granpayeh has received his B.Sc., M.Sc., and Ph.D. degrees in Telecommunication Engineering from Telecommunication College of Iran, Radio and Television Colledge, Tehran, Iran and University of N.S.W., Sydney Australia, in 1975, 1980, and 1996, respectively.

In 1975, as an honor graduate of the Faculty of Electrical and Computer Engineering of K. N. Toosi University of Technology, he was employed as an instructor there, where he was later promoted to lecturer, assistant, and associate professor in 1980, 1996, and 2007 respectively. His research interests are in optical devices, equipments and materials, optical fibers, and optical fiber nonlinear effects. He is the author or co-author of 50 journal- and 75 conference- papers. He is a member of OPSI, ISEE, IEEE, and OSA.

